Model for Polluted Insulator Flashover under AC or DC Voltage

T. Chihani, A. Mekhaldi
Laboratoire de Recherche en Electrotechnique, Ecole Nationale Polytechnique, Algiers, Algeria

A. Beroual
AMPERE Lab CNRS UMR 5005, Ecole Centrale de Lyon, University of Lyon, 36 Avenue Guy de Collongue, 69134 Ecully, France

and **M. Teguar** and **D. Madjoudj**
Laboratoire de Recherche en Electrotechnique, Ecole Nationale Polytechnique, Algiers, Algeria

ABSTRACT

The aim of this paper is to elaborate a model describing the different phases of flashover of high voltage insulators with continuous or discontinuous pollution deposits, in AC or DC. This model uses an equivalent electrical circuit. It consists of three sub-algorithms: (1) The first one is a preliminary algorithm enabling the quantification of the electrical equivalent circuit parameters based on analytical and semi-analytical formulations; (2) the second one is relative to the steady state of discharge (static sub-model), at the beginning of flashover; and (3) the third one describes the unstable mode (dynamic sub-model). The whole algorithm describes the evolution of the discharge up to flashover. It enables to determine the different parameters characterizing the discharge such as the current, length, radius, propagation velocity, linear resistance and temperature. The simulated values are found in a good agreement with the experimental ones.

Index Terms — **flashover; polluted insulators; stable regime; static model; critical conditions; unstable regime; dynamic model**

1 INTRODUCTION

FLASHOVER of high voltage polluted insulators is one of the main causes of disruption in power systems. It generally results of the development and intensification of a leakage current generated within a pollution layer deposited at the insulators surface. The distribution of this pollution layer depends on many parameters such as weather conditions, electric field, insulators catching position and insulators material [1-6]. Its severity mainly depends on the nature and source of pollutant deposits (natural, industrial or mixed) and their conductivities [7] as well as the precipitation intensity. The classification of the different types of pollution and their severities can be found in IEC and IEEE standards [8-12].

Even if the process leading to the initiation of the leakage current and its intensification up to insulator flashover is well known, we recall here the main features to better situate our work. Indeed, the humidification of pollution layer results in the dissolution of salts contained in the pollution deposit and hence the appearance of an electrolyte; the conductance of which leads to a reduction of the resistance of electrical system and establishing a leakage current. This latter will heat the pollution layer resulting in the evaporation of humidity from the pollution layer leading to the drying of some areas and gradually to the appearance of dry bands. From that moment, the current will drop at very low values and the resistance of the pollution layer becomes important; it takes high values. These dry bands modify the electrical potential distribution on the insulator and most electric field lines will concentrate in these bands [13]. If these local electrical fields are sufficiently high, electrical discharges occur bridging these dry bands. And depending on the experimental conditions, these partial discharges can either grow and cover the totality of insulator (flashover) or turn off after a time.

In DC voltage, the discharge will lengthen until covering the whole of the insulator, if the electrical conditions permit. Otherwise, the dry band will extend until the voltage will be no able to sustaining the discharge which will shut down. In AC voltage, the current wave passage by zero constitutes a particular problem. Thus, when the propagation velocity is relatively low, the passage of the current by zero occurs before

Manuscript received 15 May 2017, in final form 15 December 2017, accepted 20 December 2017. Corresponding author: T. Chihani.

DOI: 10.1109/TDEI.2017.006815

the total flashover leads to the discharge extinction. If the discharge reigniting condition is satisfied [14, 15], the discharge will be reformed again.

The discharge evolution consists of two steps. The first one is that of stable state corresponding to the beginning of flashover. During this step, the discharge maintaining depends upon the applied voltage. Once the critical conditions are satisfied [1], the discharge becomes unstable (unstable regime); this is the final jump during which the discharge will cover the entire length of insulator.

This paper deals with modeling of discharge propagating on polluted insulator surface up to flashover using an equivalent electrical circuit. A preliminary algorithm is first used to determine the electrical components of this circuit enabling to build a static model describing the stable state using a static algorithm. Then, a dynamic algorithm is proposed to describe the discharge when it enters in unstable mode resulting in flashover after some critical conditions are satisfied. This model enables to determine the main characteristic parameters of discharge such as the current, length, radius, propagation velocity, linear resistance and temperature. The linear resistance is determined by using an analytical equation we will establish in this work instead that one met in literature which uses empirical and semi empirical equations. A comparison of the computed results with the experimental ones is achieved.

2 DETERMINATION OF EQUIVALENT CIRCUIT PARAMETERS

The used equivalent electrical circuit is inspired by the one proposed by Obenaus [16]. It consists of a cylindrical discharge of axial length X_d and resistance R_d, in series with the non-crossed width of pollution layer represented by a resistance R_p in parallel with a capacitance C_p (Figure 1); the leakage length (electrode gap) being L.

The model consists of three parts. The first one is a preliminary algorithm enabling to determine the parameters of the equivalent electrical circuit. This algorithm uses the experimental values of the discharge current, applied voltage and phase angle between those last two for different discharge lengths. The values of the discharge resistance, and the resistance and capacitance of pollution layer are determined for different discharge lengths, using analytical and semi-analytical formulations. Note that when the flashover occurs, the equivalent impedance of pollution layer will be equal to zero. Using the values of parameters so calculated and an interpolation with Matlab software, we establish two equations: the first one for the resistance of pollution layer and the second one for its capacitance. The total leakage length is divided into different intervals for discharge lengths. We choose the most appropriate formulation for each interval between polynomial in different degrees, Gaussian, logarithmic, rational or power formulations. The discharge resistance is calculated from the discharge current value.

The voltage drop at the electrodes is ignored as showed by Rizk [17] and Rizk et al [18] in the calculations of critical conditions.

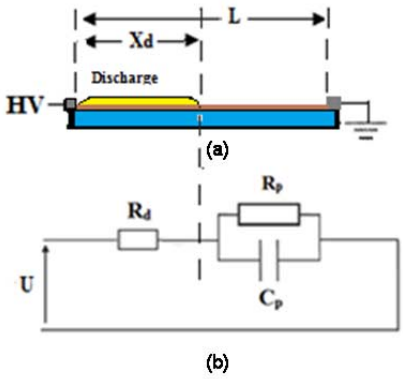

Figure 1. Model of discharge in series with the non-crossed width of pollution layer according to (a) Obenaus and (b) its corresponding electrical circuit.

Thus, the equivalent electric circuit impedance Z_{eq} is:

$$Z_{eq} = \frac{U}{I_d} \tag{1}$$

where U is the applied voltage and I_d the discharge current.

$$Z_{eq} = R_d + \frac{1}{\frac{1}{R_p} + j\omega C_p} \tag{2}$$

or

$$Z_{eq} = \left[R_d + \frac{R_p}{1+\omega^2 {C_p}^2 {R_p}^2}\right] + j\left[-\frac{{R_p}^2 C_p \omega}{1+\omega^2 {C_p}^2 {R_p}^2}\right]. \tag{3}$$

This equation can be written in the following form

$$Z_{eq} = Zp + jZq \tag{4}$$

with

$$Z_p = R_d + \frac{R_p}{1+\omega^2 {C_p}^2 {R_p}^2} \tag{5}$$

and

$$Z_q = -\frac{{R_p}^2 C_p \omega}{1+\omega^2 {C_p}^2 {R_p}^2}. \tag{6}$$

where Z_p and Z_q are respectively the real and imaginary parts of the equivalent impedance of the whole circuit. These values are determined from the module of the equivalent impedance and the phase angle between the applied voltage and the discharge current.

By dividing equation (6) by equation (5), it yields

$$R_p C_p \omega = \frac{Z_q}{R_d - Z_p} \tag{7}$$

which gives

$$C_p = \frac{1}{\omega R_p}\frac{Z_q}{(R_d - Z_p)} \tag{8}$$

and by substituting eq. (8) into eq. (5), one gets

$$Z_p - R_d = \frac{R_p}{1+\frac{{Z_q}^2}{(R_d - Z_p)^2}}. \tag{9}$$

This gives

$$R_p = \frac{(R_d - Z_p)^2 + {Z_q}^2}{Z_p - R_d}. \tag{10}$$

The discharge resistance R_d can be determined from the discharge current and length X_d by equation (11) [19]

$$R_d = \frac{AX_d}{{I_d}^{n+1}} \tag{11}$$

with A and n the flashover constants.

Generally, the radius of discharge channel is assumed to be constant and the discharge resistance is computed using Mayer's equation [20]. While in practice, it increases with the current. In our modeling, this radius is considered to be variable. Figure 2 gives the flowchart describing the different steps of computation.

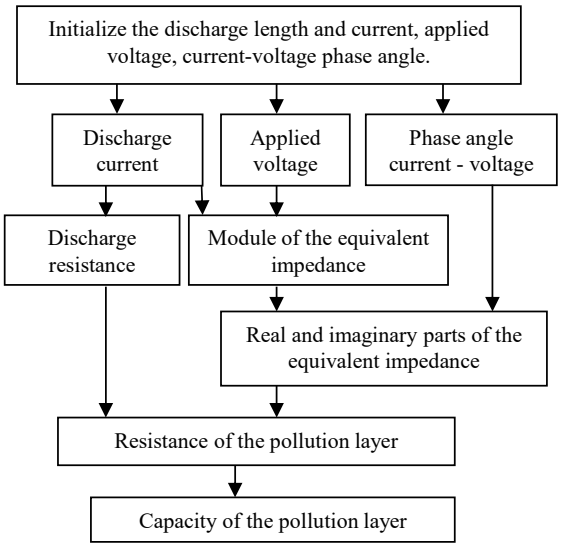

Figure 2. Chart of the equivalent electrical circuit parameters identification algorithm.

3 STATIC MODEL FOR STABLE MODE

The stable mode is the first phase of flashover. During this step, each increasing in the voltage leads to an increase in the discharge length. The different equations used in this static mode to determine the different parameters of discharge are described in the following.

In AC, the discharge reigniting condition gives [14] [15]

$$kX_d = U{I_d}^n \tag{12}$$

where k is the discharge reinitiating constant and by substituting equation (12) in equation (1), it yields

$$U = Z_{eq}\left(\frac{kX_d}{U}\right)^{\frac{1}{n}} \tag{13}$$

or,

$$U = \left(kX_d{Z_{eq}}^n\right)^{\frac{1}{n+1}}. \tag{14}$$

The equivalent impedance Z_{eq} depends on the discharge length (previous algorithm). So we can determine the different values that this last takes for a given voltage value.

In DC, there is no capacitive effect. Thus, the voltage across the system will be

$$U = (R_d + R_p)I_d \tag{15}$$

R_p and R_d being respectively

$$R_p = \rho_p \frac{(L-X_d)}{S_p} \tag{16}$$

and

$$R_d = \rho_d \frac{X_d}{S_d} \tag{17}$$

where ρ_p and ρ_d are the resistivities of pollution layer and discharge channel, respectively. Thus the linear resistance of pollution layer r_p and discharge channel r_d will be, respectively

$$r_p = \frac{\rho_p}{S_p} \tag{18}$$

and

$$r_d = \frac{\rho_d}{S_d}\ . \tag{19}$$

According to the impedance criterion established by Dhahbi *et al* [21], the critical case of discharge propagation is

$$\frac{\rho_p}{S_p} = \frac{\rho_d}{S_d} \tag{20}$$

or

$$r_p = r_d. \tag{21}$$

And from equations (16), (17) and (20), it yields

$$\frac{R_p}{(L-X_d)} = \frac{R_d}{X_d}. \tag{22}$$

By substituting equation (22) into equation (15), one can write

$$U = \frac{L}{X_d}R_d I_d \tag{23}$$

and by using equation (11), the voltage at the discharge will be

$$U_d = R_d I_d = \frac{AX_d}{{I_d}^n}. \tag{24}$$

After arrangement of equation (22) and equation (24), it comes

$$R_p\left(\frac{X_d}{(L-X_d)}\right) = \frac{AX_d}{{I_d}^{n+1}} \tag{25}$$

that gives

$${I_d}^{n+1} = \frac{A(L-X_d)}{R_p}\ . \tag{26}$$

So, the current I_d will be

$$I_d = A^{\frac{1}{n+1}}\left(\frac{(L-X_d)}{R_p}\right)^{\frac{1}{n+1}} \tag{27}$$

and by substituting I_d in equation (23) and by using equations (22) and (27) we will have

$$U = \frac{L}{(L-X_d)}R_p A^{\frac{1}{n+1}}\left(\frac{(L-X_d)}{R_p}\right)^{\frac{1}{n+1}}. \tag{28}$$

That is to say,

$$U = LA^{\frac{1}{n+1}}\left(\frac{R_p}{(L-X_d)}\right)^{\frac{n}{n+1}}. \tag{29}$$

By using the first algorithm, one determines the resistance of pollution layer versus the discharge length. This later is determined by equation (29), for different voltage values.

To compute the discharge radius, one uses the following relationship [22]:

$$a_d = \sqrt{\frac{I_d}{1.45\pi}}. \quad (30)$$

To compute the discharge temperature, one assumes that the total energy is dissipated by thermal conduction within the discharge channel [23]. Thus, according to Fourier's law, one can write the relationship giving this energy *P* per unit length:

$$\mathrm{P} = E_d I_d = \frac{dQ}{dt} = -\lambda_{th} A_{iso} \frac{\partial T_d}{\partial u_n} \quad (31)$$

where E_d, I_d, Q, λ_{th}, A_{iso}, u_n and T_d are respectively the voltage gradient in the discharge, the discharge current, heat quantity, thermal conductivity, isothermal surface element in the discharge, the normal direction of the temperature gradient in the discharge and the axial temperature required for thermal ionization.

By assuming (1) the isothermal surfaces of the discharge channel to be hemispherical and the temperature propagation equation to be uni-dimensional and (2) the discharge is in a local thermodynamic equilibrium (i.e.; there is no temperature or pressure gradient between the different parts of the system and there is no variation of the chemical composition), the energy balance will be [23]:

$$P = E_d I_d = \pi \lambda_{th} T_d. \quad (32)$$

According to Ohm's law

$$E_d = \rho_d J_d = \frac{I_d}{\sigma_d S_d} \quad (33)$$

where σ_d, S_d, ρ_d and J_d are respectively the discharge conductivity, section, resistivity and current density.

By combining equations (19), (32) and (33) one can write:

$$T_d = \frac{r_d {I_d}^2}{\pi \lambda_{th}} \quad (34)$$

where the linear resistance of the discharge, r_d,, is given by equation (24):

$$r_d = \frac{A}{{I_d}^{n+1}} \ . \quad (35)$$

Thus, by substituting equations (35) in (34), it comes:

$$T_d = \frac{A}{\pi \lambda_{th} {I_d}^{n-1}}. \quad (36)$$

Generally, to characterize the dynamic evolution of the discharge linear resistance, many authors use Mayer's equation [20] that is,

$$\frac{1}{\mathrm{r_d}} \frac{\mathrm{dr_d}}{\mathrm{dt}} = \frac{1}{\tau}\left(1 - \frac{\mathrm{r_d {I_d}^2}}{\mathrm{P_0}}\right). \quad (37)$$

This equation is not valid in the static case. It also assumes that the discharge radius is constant what is in contradiction with the equation (30) that corresponds to the reality.

On the other hand, from equation (3), one can write the modulus of equivalent impedance of the system

$$|Z_{eq}| = \sqrt{\left[R_d + \frac{R_p}{1+\omega^2 {C_p}^2 {R_p}^2}\right]^2 + \left[\frac{{R_p}^2 C_p \omega}{1+\omega^2 {C_p}^2 {R_p}^2}\right]^2}. \quad (38)$$

By substituting equations (1) and (38) in equation (34), and knowing that the discharge linear resistance, r_d, is equal to discharge resistance, R_d, divided by discharge length, X_d, we get

$$T_d = \frac{R_d U^2}{\pi \lambda_{th} X_d |Z_{eq}|^2} \quad (39)$$

or

$$\left[R_d + \frac{R_p}{a}\right]^2 + \left[\frac{{R_p}^2 C_p \omega}{a}\right]^2 = \frac{R_d U^2}{\pi \lambda_{th} T_d X_d} \quad (40)$$

with

$$a = 1 + \omega^2 {C_p}^2 {R_p}^2 \ . \quad (41)$$

Finally, we will have a quadratic equation (polynomial) where the unknown is the discharge resistance R_d

$$\boldsymbol{R_d}^2 + \left[2\frac{R_p}{a} - \frac{U^2}{\pi \lambda_{th} T_d X_d}\right] \boldsymbol{R_d} + \frac{{R_p}^4 {C_p}^2 \omega^2 + {R_p}^2}{a^2} = 0 \quad (42)$$

and the discriminant Δ of this equation is

$$\Delta = \left[2\frac{R_p}{a} - \frac{U^2}{\pi \lambda_{th} T_d X_d}\right]^2 - 4\left[\frac{{R_p}^4 {C_p}^2 \omega^2 + {R_p}^2}{a^2}\right] \ . \quad (43)$$

Thus, the two solutions of equation (42) are

$$R_{d1} = \frac{1}{2}\left[\left[\frac{U^2}{\pi \lambda_{th} T_d X_d} - 2\frac{R_p}{a}\right] - \sqrt{\left[2\frac{R_p}{a} - \frac{U^2}{\pi \lambda_{th} T_d X_d}\right]^2 - 4\left[\frac{{R_p}^4 {C_p}^2 \omega^2 + {R_p}^2}{a^2}\right]}\right] \quad (44)$$

and

$$R_{d2} = \frac{1}{2}\left[\left[\frac{U^2}{\pi \lambda_{th} T_d X_d} - 2\frac{R_p}{a}\right] + \sqrt{\left[2\frac{R_p}{a} - \frac{U^2}{\pi \lambda_{th} T_d X_d}\right]^2 - 4\left[\frac{{R_p}^4 {C_p}^2 \omega^2 + {R_p}^2}{a^2}\right]}\right]. \quad (45)$$

When the flashover occurs, we will have

$$X_d = L \quad U = U_c \quad R_p = 0$$

U_c being the flashover voltage.

In these conditions

$$R_{d1} = 0\ \Omega/m \quad (46)$$

and

$$R_{d2} = \frac{{U_c}^2}{\pi \lambda_{th} T_d L} \ . \quad (48)$$

Thus, the corresponding linear resistances will be

$$r_{d1} = 0\ \Omega/m \quad (49)$$

and

$$r_{d2} = \frac{{U_c}^2}{\pi \lambda_{th} T_d L^2} \ . \quad (50)$$

In the first case ($r_{d1} = 0$), the current and temperature will be infinite which is not realistic. By using the second solution r_{d2} ($r_{d2} \neq 0$), and by substituting it in equation (39), one can write

$$T_d = \frac{{U_c}^2}{\pi \lambda_{th} r_d L^2} \ . \quad (51)$$

Knowing that $R_d = r_d L$ and $I_d = \frac{U_c}{R_d}$, it yields

$$T_d = \frac{r_d {I_d}^2}{\pi \lambda_{th}}. \quad (52)$$

This relationship is consistent with equation (34) we established above. In consequence, we keep R_{d2} as the solution of equation (42). Thus the linear resistance of discharge we use in the following, will be $r_d = r_{d2}$

$$r_d = \frac{1}{2X_d}\left[\left[\frac{U^2}{\pi\lambda_{th}T_d X_d} - 2\frac{R_p}{a}\right] + \sqrt{\left[2\frac{R_p}{a} - \frac{U^2}{\pi\lambda_{th}T_d X_d}\right]^2 - 4\left[\frac{{R_p}^4 {C_p}^2 \omega^2 + {R_p}^2}{a^2}\right]}\right] \quad (53)$$

In DC, this equation will be reduced to

$$r_d = \frac{1}{2X_d}\left[\left[\frac{U^2}{\pi\lambda_{th}T_d X_d} - 2R_p\right] + \sqrt{\left[2R_p - \frac{U^2}{\pi\lambda_{th}T_d X_d}\right]^2 - 4{R_p}^2}\right]. \quad (54)$$

This relationship is an analytical one contrary to the relationship met in literature which uses empirical and semi empirical equations. Figure 3 depicts the flow chart of this static mode.

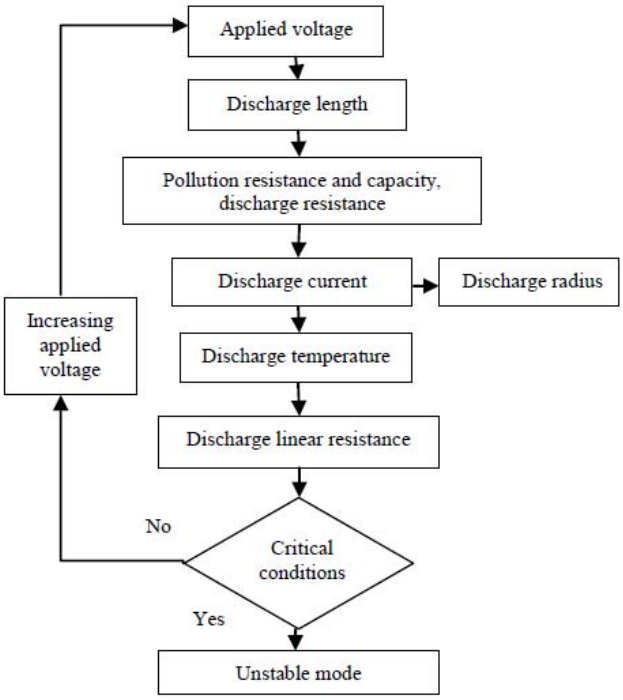

Figure 3. Chart of static model.

4 DYNAMIC MODEL FOR THE UNSTABLE MODE

Once the flashover critical conditions are reached, the discharge enters in the unstable mode resulting in the final jump and the overlap of the entire leakage length. This mode is described by a dynamic model. The initial values of this dynamics are the final values of the static model which describes the previous phase of flashover. For this dynamics model, the used propagation criterion is that one proposed by Dhahbi et al [21].

To compute the discharge propagation velocity, one uses Beroual's formula [24]

$$v_d(t) = \sqrt[3]{\frac{2\beta P_t(t)}{\rho\pi {a_d}^2}} \quad (55)$$

where β is the fraction of the whole electrical energy (power P_t) injected into the system and dedicated for the displacement of discharge; it ranges 0.05 to 0.10; ρ is the density and a_d is the discharge radius.

Concerning the discharge length, it is computed at each step dt by iteration using the dynamic model algorithm. Thus, at each iteration, the new discharge length $X_{d(i+1)} = X_{d(i)}$ will be the sum of the former length $X_{d(i)}$ and the product of the velocity $v_d(t).dt$

$$X_{d(i+1)} = X_{d(i)} + v_d(t)dt \quad (56)$$

where i is the iteration number.

Figure 4 gives the flow chart of the dynamic model.

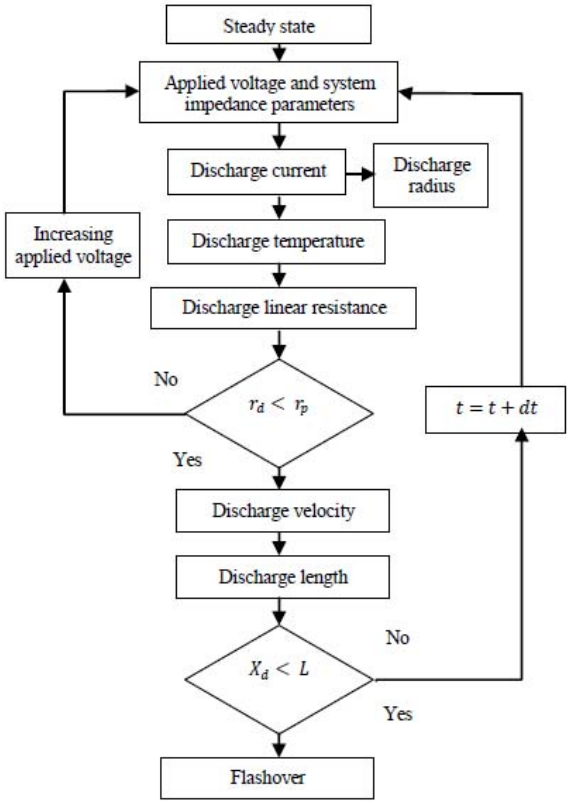

Figure 4. Chart of dynamic model.

5 EXPERIMENT AND VALIDATION OF MODELS

To validate our modelling, we compare the experimental values of the discharge length versus the voltage under AC with those computed using equation (14) for the characteristic applied voltage – discharge length and equation (1) for discharge current.

The experiments are carried out in the high voltage laboratory of the Ecole Nationale Polytechnique of Algiers,

Algeria. The experimental setup consists of a test transformer (500 V/300 kV, 50 kVA, 50 Hz), camera SONY DCR-SR for visualization of the flashover evolution and numerical oscilloscope connected to computer for recording the voltage and the leakage current.

The insulator model is a glass plate (500×500×5 mm) covered with a humidified sand. The electrodes consists of two aluminum foil bands (500×3×0.003 mm); one is connected to the tests transformer and the other to the ground. The total leakage length (distance between both electrodes) is of 292 mm. Figure 5 gives an overview of the experimental device.

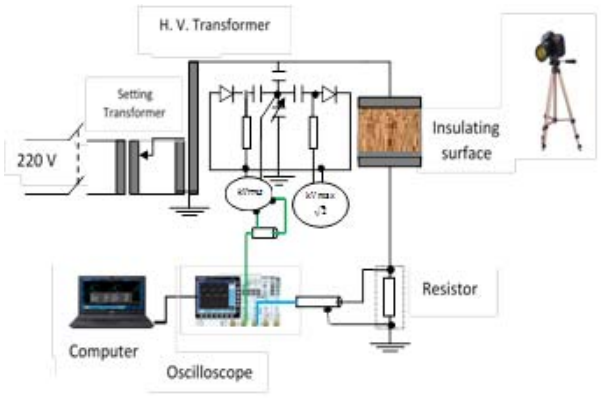

Figure 5. General view of experimental device.

The used pollution layers consist of sand originate from two algerian Sahara desert regions. The first one is from Bechar situated in the South West of Algeria, the surface conductivity of which is 30 nS for a NSDD of 0.0308 g/cm^2 and the second one from Boussaada which is in the South East of Algeria, the surface conductivity of which is 23 nS for a NSDD of 0.0205 g/cm^2. The sand layers are moistened with a spray of 15 ml of distilled water.

Figures 6 and 7 present the experimental characteristics of the applied voltage and the current versus the discharge length, as well as the simulated results obtained by our model, respectively for both types of sands. The simulations are achieved using Matlab 2015a software. One observes a good accordance between the experimental and simulated results. Thus, one can consider that our model works well. It will be used in the folowing to compute the other characteristic parameters of discharge up to flashover.

6 SIMULATIONS AND RESULTS

6.1 DISCHARGE LENGTH

During the stable mode, the voltage is gradually increased from 10 to 90 kV for insulator covered with Boussaada sand and from 10 to 98 kV for insulator covered by Bechar sand. It is observed that the discharge extends progressively to reach the critical length that is 12.3 cm corresponding to 90 kV for Boussaada Sand and 15.9 cm corresponding to 98 kV for Bechar sand (Figure 8). The difference in the critical values of discharge length and applied voltage between both cases is due to the differences in the sand characteristics (i.e.; chemical composition). The electrolyte with constituents of Bechar sand

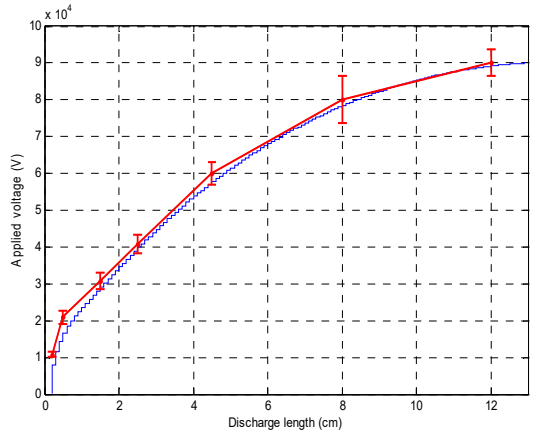

(a)

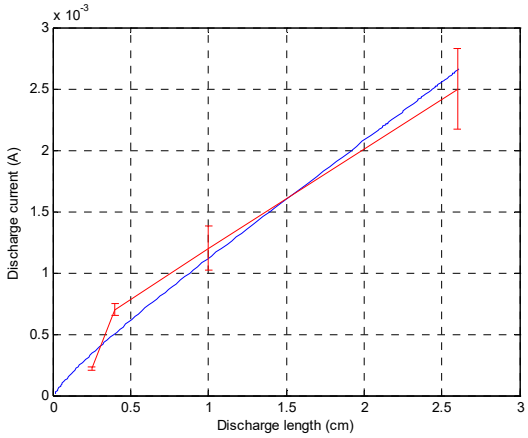

(b)

Figure 6. Applied voltage (a) and current (b) verses discharge length for Bechar sand. Experimental results in red and simultaed results in blue.

has higher conductivity than the other one. When the critical conditions are satisfied, the discharge will enter in the unstable mode and will have a dynamic evolution up to cover the whole leakage length (Figure 9).

6.2 DISCHARGE CURRENT

Figure 10 shows the evolution of the current versus the discharge length. One observes that the current gradually increases for both types of pollution in the first 2/3 of the total leakage length L; and in the last third of L which corresponds to the unstable mode described by the dynamic model, the current sharply increases up to flashover. When the discharge propagates, the pollution impedance decreases as well as the discharge resistance. Over the half of total leakage length, the current with Bechar sand is higher than that with Boussaada sand. The current behavior depends on applied voltage as well as pollution layer conductivity. Thus, the difference in these influencing parameters for the two cases (Bechar sand and Bousaada) leads to different evolutions for discharge current during flashover.

6.3 DISCHARGE RADIUS

The discharge radius depends on the discharge current (see equation (30)). It increases progressively in the first 2/3 of the

total leakage length while it sharply increases in the last third of L, for both types of sand (Figure 11). However, it is larger with Bechar sand.

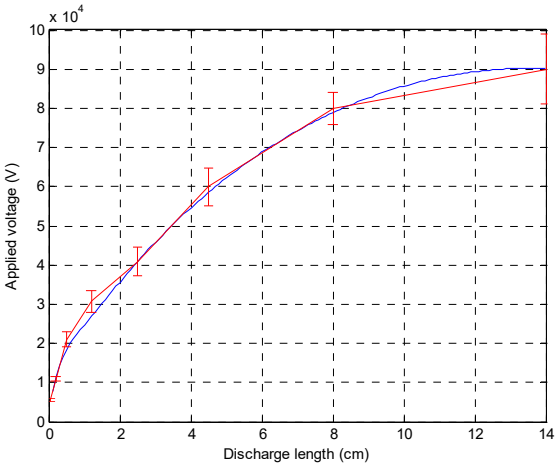

(a)

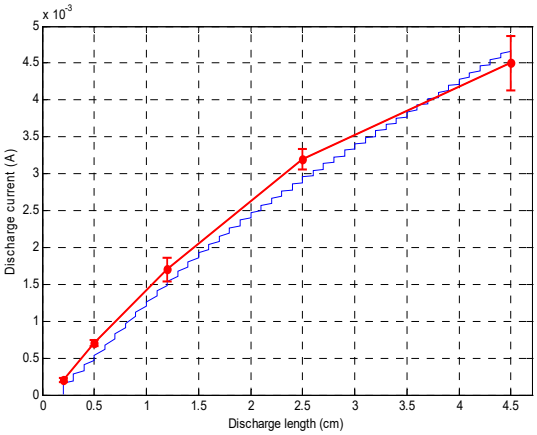

(b)

Figure 7. Voltage (a) and current (b) verses discharge length for Boussaada sand. Experimental results in red and simultaed results in blue.

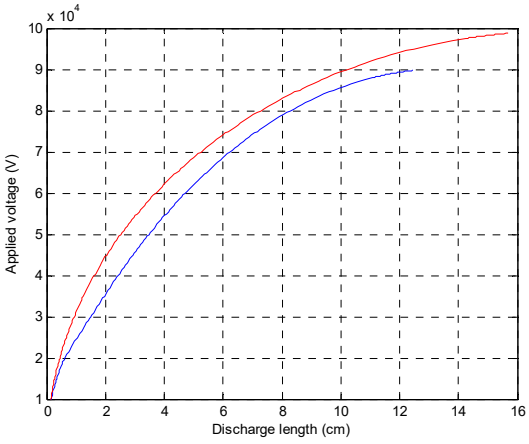

Figure 8. Applied voltage verses discharge length during the stable mode; Bechar sand (red) and Bousaada sand (blue).

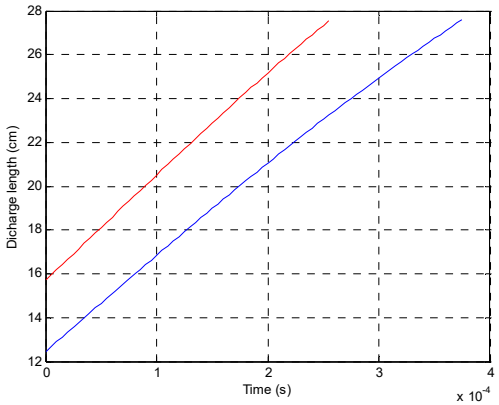

Figure 9. Temporal evolution of the discharge length during the unstable mode; Bechar sand (red) and Bousaada sand (blue).

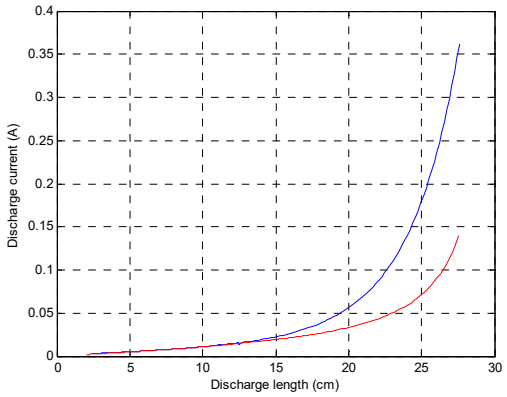

Figure 10. Discharge current verses discharge length; Bechar sand (red) and Bousaada sand (blue).

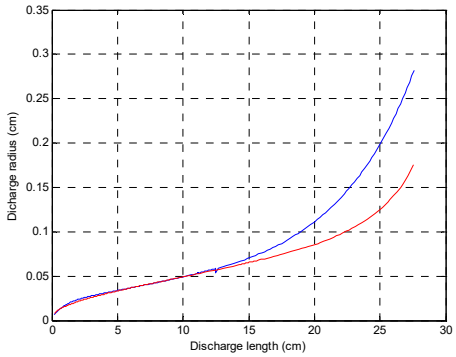

Figure 11. Discharge radius verses discharge length; Bechar sand (blue) and in Bousaada sand (red).

6.4 DISCHARGE TEMPERATURE

The increase of discharge current leads to an increase of temperature within the discharge channel and in its vicinity (Figure 12). The computed temperature are in the same range as those reported in literature [25-27].

6.5 DISCHARGE LINEAR RESISTANCE

When the discharge starts propagating, its linear resistance r_d sharply decreases as it is observed (Figure 13); with Bechar sand, r_d loses 95% of its value when the discharge length passes from 2 to 10 cm. Then, it gradually decreases up to flashover. This decrease obeyes to Dhahbi et al propagation criterion [22] and Fridman et al equation [28].

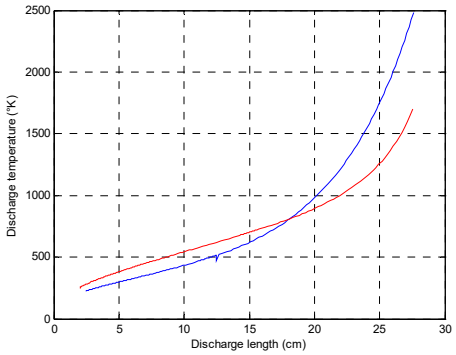

Figure 12. Discharge temperature verses discharge length; Bechar sand (red) and in Bousaada sand (blue).

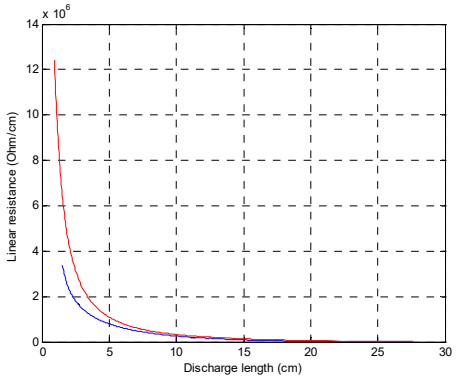

Figure 13. Discharge linear resistance verses discharge length; Bechar sand (red) and Bousaada sand (blue).

6.6 DISCHARGE PROPAGATION VELOCITY

Figure 14 gives the evolution of the discharge propagation velocity versus the discharge length. We observe that during the stable regime (before 12.3 cm for Bousaada case, and before 15.9 cm for Bechar case), the discharge is in a static mode. After then, the discharge enters in unstable regime (i.e.; dynamic evolution) and its velocity very sharply increases reaching some hundreds of m/s.

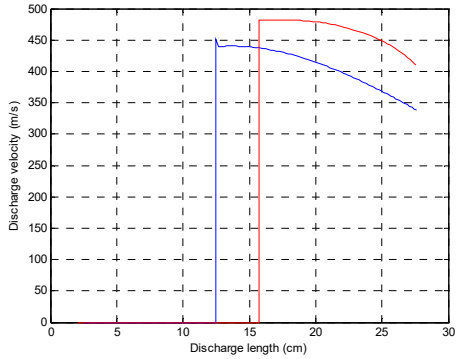

Figure 14. Discharge propagation velocity verses discharge length; Bechar sand (red) and in Bousaada sand (blue).

7 CONCLUSIONS

The developed model constitutes a helpful tool for characterizing the different phases of discharge propagating over polluted insulator under AC and DC, up to flashover. It is based on an equivalent electrical circuit and analytical and semi-analytical formulations. It enables to compute the main characteristic parameters of discharge and their evolution depending on the experimental conditions.

An analytical relationship enabling to determine the discharge linear resistance versus the discharge temperature, applied voltage, discharge length and pollution parameters, was established. While the relationship reported in literature and used till today has been established basing on empirical and semi empirical formulations.

It is showed that the type of pollution layer influences the electrical current and hence the evolution of the radius, linear resistance and temperature of discharge channel.

REFERENCES

[1] M. Farzaneh and W. A. Chisholm, *Insulators for icing and polluted environments*, IEEE Press, John Wiley & Sons, Inc. Publication, 2009.

[2] M. Akbar and F. Zedan, "Performances of HV transmission line insulators on desert conditions - Part 3: pollution measurement at a coastal site in the eastern region of Saudi Arabia", IEEE Trans. Pwr. Del., vol. 6, no. 1, pp 429-438, 1991.

[3] M. El-A. Slama, "Contribution à l'étude de l'influence de la non-uniformité de la distribution de la pollution basée sur la méthode de la DDSE pour le dimensionnement des isolateurs des lignes THT a courant alternatif". Thèse de Magister, Université des Sciences et Technologies d'Oran (USTO), Algerie, 2002 (in French).

[4] K. Takasu, T. Shindo and N. Arai, "Natural contamination test of insulators with DC voltage energization at Inland Areas", IEEE Trans. Pwr. Del, vol. 3, pp 1847-1853, 1988.

[5] K. Naito, K. Morita, Y. Hasegawa and T. Imakoma, "Improvement on the DC voltage insulation efficiency of suspension insulators under contaminated conditions", IEEE Trans. Electr. Insul., vol. 23, pp. 1025-1032, 1988.

[6] X. Lin, Z. Chen, X. Liu, K. Chu, K. Morita, R. Matsuoka and S. Ito, "Natural insulator contamination test results on various shed shapes in heavy industrial contamination areas", IEEE Trans. Electr. Insul., vol. 27, pp. 593-600, 1992.

[7] Publication IEC 71-12 "Insulation coordination application guide", Seconde édition, 1976.

[8] Cigre working group 33-04, "The measurement of site pollution severity and its application to insulator dimensioning for AC systems," GT/WG 04. Electra, N°20, 1979.

[9] CEI 60507, "Essais sous pollution artificielle des isolateurs destines aux reseaux a courant alternatif", 1991

[10] CEI 60-1, "Techniques d'essais a haute tension. Partie 1 : Definitions et prescriptions relatives aux essais", 1989.

[11] IEEE Standard Techniques for High-Voltage Testing. IEEE Std 4-1995. [18] M. K. H. Schneider "A critical comparison of artificial pollution test methods for HV insulator", GT/WG 04, Electra n°20, 1979.

[12] CEI 815, "guide pour le choix des isolateurs sous pollution," 1986.

[13] H. Hadi, "Mécanismes de contournement et sa modélisation dynamique appliquée aux isolateurs réels", Thèse de doctorat d'état, Université des Sciences et Technologies d'Oran (USTO), Algerie, 2002

[14] S. Farokhi, M. Farzaneh and I. Fofana, "Experimental Investigation of the Process of Arc Propagation over an Ice Surface", IEEE Trans. Dielectr. Elect. Insul., vol. 17, no. 2, pp.458-464, 2010.

[15] C. Volat, M. Farzaneh and N. Mhaguen, "Improved FEM Models of One- and Two-arcs to Predict AC Critical Flashover Voltage of Ice-covered Insulators", IEEE Transactions on Dielectrics and Electrical Insulation, vol. 18, no. 2, pp. 393 – 400, 2011

[16] F. Obenaus, "Fremdschichtüberschlag und Kreichweglänge," Deutsche Elektrotechnkik, vol. 4, pp. 135 – 136, 1958.

[17] F. Rizk, "Mathematical Models for Pollution Flashover", Electra, Vol. 78, pp. 71-103, 1981.

[18] F. A. M. Rizk and D. H. Nguyen, "Digital Simulation of Source Insulator Interaction in HVDC Pollution Tests", IEEE Trans. on Pwr. Del., vol. 3, no. 1, pp. 405-410, 1988.

[19] S. M. Ale-Emran and M. Farzaneh, "Flashover Performance of Ice-covered Post Insulators with Booster Sheds Using Experiments and Partial Arc Modeling", IEEE Tran. Dielectr. Electr. Insul., vol. 23, no. 2, pp. 987–994, 2016

[20] S. Taheri, M. Farzaneh and I. Fofana, "Improved Dynamic Model of DC Arc Discharge on Ice-covered Post Insulator Surfaces," IEEE Trans. Dielectr. Electr. Insul., vol. 21, no. 2, pp. 729 – 739, 2014
[21] N. Dhahbi-Megriche, A. Beroual and L. Krahenbuhl, "A New Proposal Model for Polluted Insulators Flashover", J. Phys. D. Appl. Phys., vol. 30, no. 5, pp. 889-894, 1997.
[22] R. Wilkins, "Flashover Voltage of HV Insulators with Uniform Surface Pollution Films", Proc IEE, vol. 116, pp. 457-465, 1969.
[23] El-A Slama, M. Beroual, A. Hadi, H. "Analytical computation of discharge characteristic constants and critical parameters of flashover of polluted insulators," Trans. Dielectr. Electr. Insul., vol. 16, 1764–1771, 2010.
[24] A. Beroual A. "Electronic gaseous process in the breakdown phenomena of dielectric liquids", J. Appl. Phys. 73 (9), pp. 4528-4533, 1993.
[25] S. Anjana and C. S. Lakshminarasmha, "Computed of Flashover Voltages of Polluted Insulators Using Dynamic Arc Model" in *Proceedings of the 6th International Symposium on High Voltage Engineering*, 1989.
[26] T. Matsumoto; M. Ishii; T. Kawamura. "Optoelectronic Measurement of Partial Arcs on a Contaminated Surface", IEEE Trans. Dielectr. Electr. Insul., vol. 19, pp. 543–549, 1984.
[27] F. Hadjrioua; D. Mahi; M. El-A. Slama, "Electro-thermal dynamic model using the analytical arc parameters for the prediction of the critical flashover condition on the HVDC polluted insulator", IET Generation, Transmission & Distribution, vol. 10, pp. 427–436, 2017.
[28] A. Fridman et al, "*Gliding arc discharge",* Progress in Energy Combustion Science 25, Elsevier Sciences Ltd, pp. 211-231, 1999.

Tarek Chihani was born in Cherchell, Algeria in 1991. He received the degree of Engineer and Masters in Electrical Engineering from Ecole Nationale Polytechnique of Algiers in 2013. He is currently a PhD student at the Electrical Engineering Department in the same engineering school. His research areas include outdoor insulators pollution, modeling of insulators flashover and renewable power.

Abdelouahab Mekhaldi (M'04, S'06) received the degree of Engineer in 1984 in Electrical Engineering, Master degree in 1990 and Ph.D in High Voltage Engineering in 1999 from the Ecole Nationale Polytechnique (ENP) of Algiers. He is currently Professor at ENP. His main research areas include discharge phenomena, outdoor insulators, polymeric cables insulation, lightning, artificial intelligence application in high voltage insulation diagnosis and electric field computation.

Abderrahmane Beroual (F'11) is currently Professor at the Ecole Centrale de Lyon, University of Lyon, France. Presently, he is the head of High Voltage Group at AMPERE Lab – CNRS and scientific expert at SuperGrid Institute; he is also responsible of the Master Research Program in electrical engineering. From 1994 to 1998, he chaired the International Study Group on Streamer Propagation in Liquids of the IEEE – DEIS. He is member of many Advisory Committees of International Conferences, Technical Committee of the IEEE CEIDP, UF10 Technical Commission – MT30 of IEC and associate editor for IEEE TDEI. He was the recipient of the 2016 IEEE T. Dakin Award. His main research interests include high voltage insulation, outdoor insulation, dielectric materials, long air gaps discharge and lightning, modelling of discharges and composite materials. He supervised more than 45 PhD theses. He is author/co-author of more than 430 technical papers including more than 170 refereed journal papers, 5 patents, two books and 5 book chapters.

Madjid Teguar obtained a first degree in Electrical Engineering in 1990, Master degree in 1993 and Ph.D in High Voltage Engineering in 2003 from the Ecole Nationale Polytechnique (ENP) of Algiers. He is now Professor in electrical engineering at ENP. His research interests include insulation systems, insulation coordination, earthing of electrical energy systems and polymeric cables insulation.

Djamal Maadjoudj was born in Batna, Algeria in 1989. He received the degree of Engineer in Electrical Engineering in 2014 from the Ecole Nationale Polytechnique (ENP) of Algiers. He is currently a PhD student at the same engineering school. His principal research include discharges phenomena and oudor insulation.